Experimental and numerical analysis of the fracture process in the splitting tension test of concrete

V. Malárics & H.S. Müller
Institute of Concrete Structures and Building Materials, University of Karlsruhe, Karlsruhe, Germany

ABSTRACT: This research project aimed for the derivation of a consistent conversion formula between splitting tensile strength $f_{ct,sp}$ and uniaxial tensile strength f_{ct} by applying methods of fracture mechanics. The derived conversion formula should encompass the entire spectrum of structural concretes used in practice. To achieve this target, an extensive experimental programme was carried out. Two normal strength, two high strength as well as two self-compacting concretes using different aggregates were tested. To analyse the obtained experimental results, the splitting tension tests and the uniaxial tension tests were modelled numerically. Both experimental and numerical test results showed that the uniaxial tensile strength f_{ct} cannot be calculated from the splitting tensile strength $f_{ct,sp}$ using a single constant conversion factor. The main reason is due to the failure mechanism of the splitting tension test. Related fracture mechanical considerations are under development.

1 INTRODUCTION

The uniaxial tensile strength f_{ct} of concrete represents an important characteristic for the design and analysis of concrete structures. To determine the concrete characteristics of existing structures, testing is usually carried out on cores. The splitting tension test, which is very popular due to its simple experimental set-up, is widely accepted in practice. In order to estimate the uniaxial tensile strength f_{ct} from the determined splitting tensile strength $f_{ct,sp}$, conversion factors are used. According to e.g. CEB-FIP Model Code 90 (1993) the uniaxial tensile strength f_{ct} is 0.9 times the splitting tensile strength $f_{ct,sp}$. Besides the fact that the values thus obtained are far too small for modern concretes, the conversion provides inconsistent values. This behaviour can be explained by the complex tensile state, which is created within the test specimen during the splitting tension test. The specimen is primarily subjected to compressive stresses in the direction of the linearly distributed load. Perpendicular to this direction tensile stresses dominate. With increasing strength, the concrete reacts more and more sensitively to such biaxial stress conditions, resulting in early failure.

First investigations on this problem were conducted in the 1950's, where the examination of the biaxial stress conditions and the criteria of failure were based on considerations according to the theory of elasticity (e.g. Zegler 1956). It could be shown, that failure in the splitting tension test can be considered as tension failure at higher values of the ratio between compressive and tensile strength, while at lower values shear failure dominates (Bonzel 1964). However, the consideration of the stress distribution in the concrete cylinder based on the theory of elasticity, did not account for plastic deformations in the area directly below the load bearing strips, where compressive stresses dominate.

Rocco et al. (1999a) analysed the effect of specimen size and load bearing strip width on the determined splitting tensile strength in the splitting tension test. They found that the splitting tensile strength notably decreases with increasing specimen size. On the other hand, wider load bearing strips lead to an increase of the value of the splitting tensile strength. Later the experimental investigations were analysed numerically using the Fictitious Crack Model implemented in a FE-code (Rocco et al. 1999b). The calculations showed the same tendency as the experiments did. However, quantitatively there were significant differences between the experimental and the numerical results. This can be traced back to the simplified description of the fracture behaviour of concrete that had been applied. For the discretisation of the crack path, interface elements were used, whose failure criterion was described as the reaching of the uniaxial tensile strength by the tensile stresses. This criterion does not take into account the strength reducing influence of the prevailing biaxial stress state. Based on the experimental and numerical results, Rocco et al.

(1999b, 2001) deduced an analytical relation to describe the correlation between the splitting and the uniaxial tensile strength depending on specimen size. Furthermore, the characteristic length l_{ch} of concrete was implemented in the model as an additional parameter. As the corresponding experimental investigations were carried out only on one type of concrete, the overall quality of the developed correlation for a wide range of concrete compositions could not be verified.

Using test results available from the literature, Arıoğlu et al. (2006) derived a relation between the compressive strength and the splitting tensile strength valid for concretes with a compressive strength up to 120 MPa. They showed that if the tensile and the compressive strength are known, the triaxial behaviour of concrete can be determined using the failure criterion by Johnson. However, they neglected the influence of, amongst others, the age at testing, the sealing and the composition of the concretes. Futhermore, the uniaxial tensile strength was calculated from the splitting tensile strength with the constant conversion factor of 0.9 in accordance with CEB-FIP Model Code 90 (1993).

The main disadvantage of correlations like the one of Arıoğlu et al. (2006), which rely on a purely empirical approach, is their statistical nature. Hence, the mathematical function deduced lacks a physical and mechanical sound basis which is inevitable to either increase the prediction accuracy by considering the influence of diverse parameters or to derive a closed formula.

2 EXPERIMENTAL INVESTIGATIONS

2.1 *Experimental programme, preparation of specimens, test set-up*

In order to obtain data for the derivation of a conversion formula, experiments consisting of compression, splitting and uniaxial tension tests were carried out. The comprehensive experimental programme incorporated concretes with different classified strength categories (C20/25, C40/50, C70/75, C100/115) as well as two self-compacting concretes (C45/55) with different aggregates (gravel and crushed aggregates).
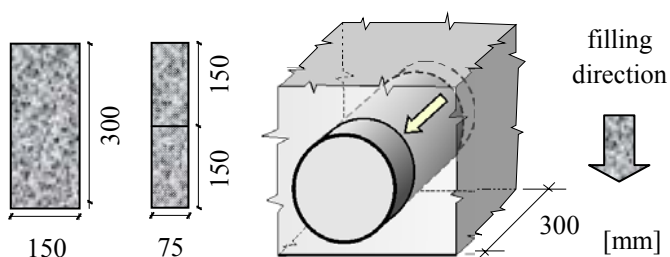

Figure 1. Dimensions of specimens for the splitting tension tests: formed specimen (left), cores (centre), extraction of core (right).
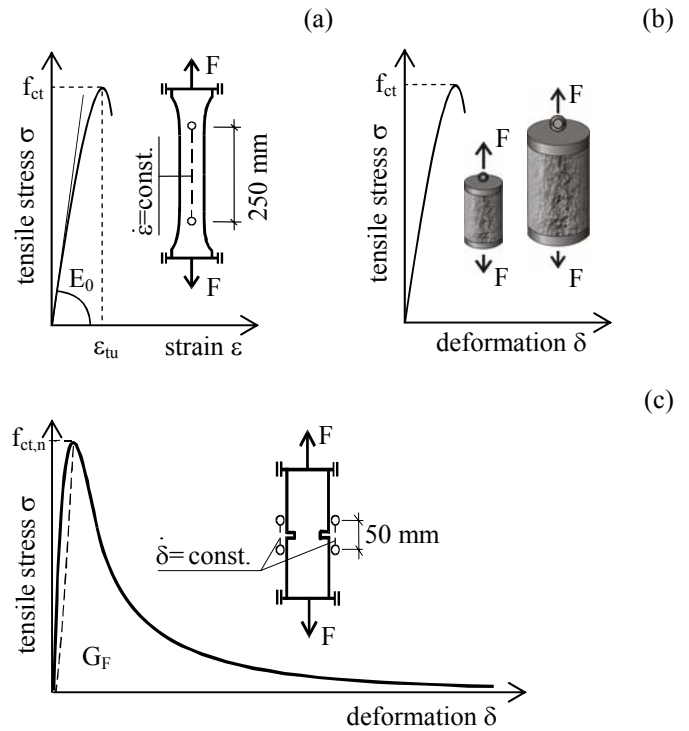

Figure 2. Geometry of unnotched dog-bone shaped prisms (a) and cores (b) as well as notched prisms (c) with illustration of the typical gradient progression and indication of characteristic concrete properties.

The compressive strength f_c was determined on cubes with an edge length of 150 mm, cylinders with a diameter D of 150 mm and a height H of 300 mm as well as cores with a diameter of 150 mm and a height of 300 mm. For each type of specimen, both normal strength and high strength concretes were used.

The splitting tension tests were performed on cylinders with varying geometries and concreting methods. On site, the characteristic values of existing concrete structures can only be determined by taking core samples. Therefore, cores with D/H = 150/300 mm/mm and D/H = 75/150 mm/mm were used. Moreover, specimens with D/H = 150/300 mm/mm, cast in accordance with DIN EN 12390-6 (2001) in cylindrical formworks, were tested.

For the uniaxial tension tests, specimens with different prism and core geometries were chosen. The concrete tensile strength f_{ct}, the tangent modulus of elasticity E_0 as well as the ultimate strain ε_{tu} were determined on dog-bone shaped prisms (see Fig. 2a). In order to record the complete stress-deformation relation, notched prisms were used (see Fig. 2c). With notches sawed 20 mm in depth and 5 mm in width in the middle of the test specimens, the resulting cross section corresponded to the cross section of the dog-bone shaped prisms (100 x 60 mm²). Taking into account a possible influence of the filling direction, the uniaxial tensile strength f_{ct} was additionally determined on cores (see Fig. 2b) according to Figure 1.
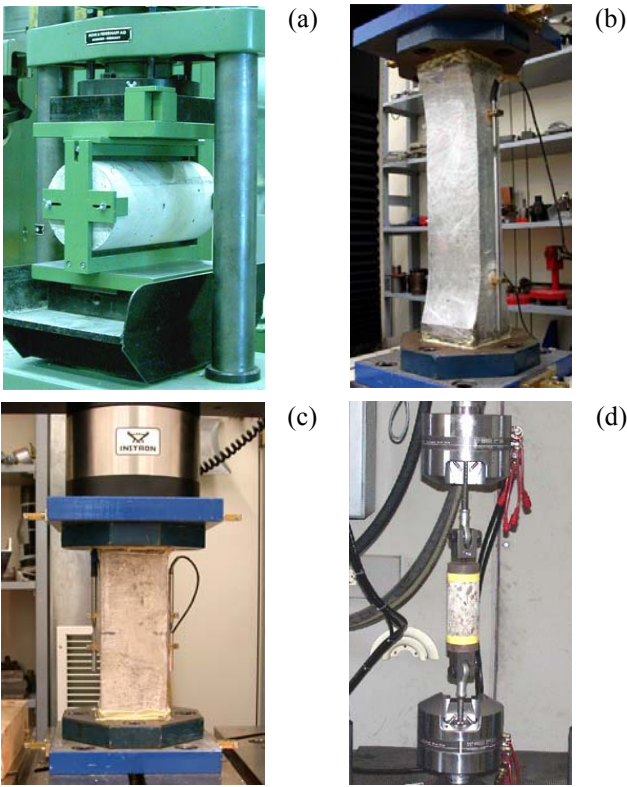
Figure 3. Centering device for splitting tension tests (a). Setup of the uniaxial tension tests on dog-bone shaped prisms (b), notched prisms (c) and cores (d).

In order to ensure the comparability of the obtained test results, a storage method equivalent to the standardized method of storage in water (DIN EN 12390, 2001) was used. A relative humidity of at least 95 % and an air temperature of 20 °C could be guaranteed by storing specimens in a covered tray with a water level of 1 cm. The cores were taken from concrete walls (see Fig. 1) at the age of approx. one week and subsequently stored as mentioned above. The specimens for tension tests were sealed 24 hours before testing with a thin polyethylene foil

and their front surfaces were impregnated with epoxy resin. All tests were carried out at a concrete age of 28 days.

The testing of splitting tensile strength $f_{ct,sp}$ was accomplished without load bearing strips, using a centering device (see Fig. 3a), according to DIN EN 12390-6 (2001). Thus, both the centrical sample installation and the load application along parallel surface lines of the core could be ensured.

This method had to be used because preliminary tests had revealed that high strength specimens (C80/95 and higher) could drop out of the testing machine due to early failure of the hard masonite plates that had to be used according to the standard (DIN EN 12390, 2001).

In order to assure uniform tension over the whole cross section during uniaxial tension testing, rigid load application plates with a thickness of 35 mm were glued to both face sides of the tension specimens.

The tests were performed with nonrotatable boundaries on dog-bone shaped prisms with a strain rate of $\dot{\varepsilon} = 0.06$ %/min and notched prisms with a deformation rate of $\dot{\delta} = 3 \cdot 10^{-2}$ mm/min. In contrast, the cores were tested with rotatable boundaries and a load application rate of 0.05 N/mm^2·s in accordance with DIN 1048 (1991) and RILEM CPC7 (1975).

2.2 Results of experimental investigations

Figure 4 represents the relation between the compressive strength f_c and the ratio of uniaxial tensile strength f_{ct} to splitting tensile strength $f_{ct,sp}$ for different kinds of specimens. Values for f_{ct} were determined on dog-bone shaped prisms whereas data for $f_{ct,sp}$ were obtained from cylinders and cores of different geometries.

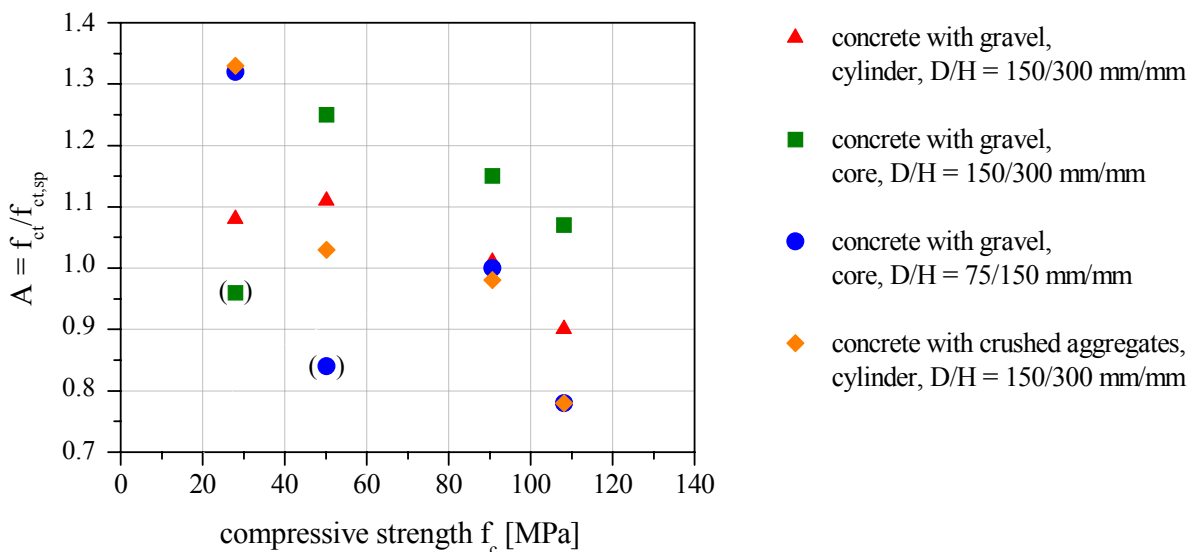The results of the experimental investigations

▲ concrete with gravel,
cylinder, D/H = 150/300 mm/mm

■ concrete with gravel,
core, D/H = 150/300 mm/mm

● concrete with gravel,
core, D/H = 75/150 mm/mm

◆ concrete with crushed aggregates,
cylinder, D/H = 150/300 mm/mm

Figure 4. Influence of the concrete strength on the ratio A of uniaxial tensile strength f_{ct} to splitting tensile strength $f_{ct,sp}$ for different kinds of specimens; stragglers in parentheses.
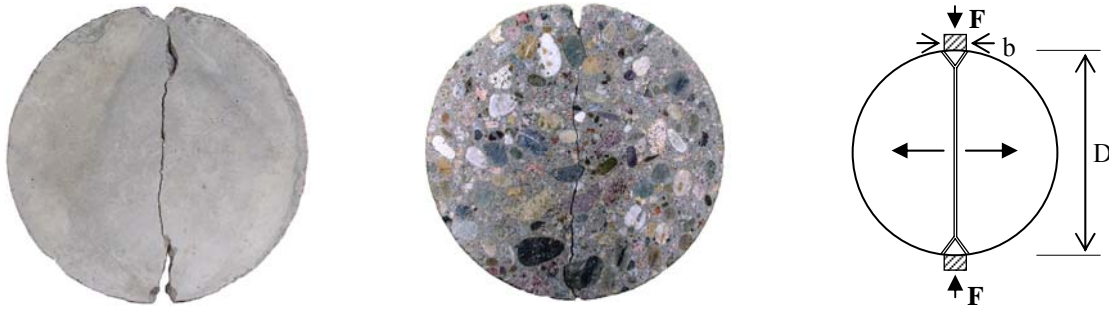
Figure 5. Fracture images of a normal strength concrete with gravel aggregate (left and centre, C40/50) and schema of the fracture mechanism (right).

Figure 6. Fracture images of a high strength concrete with gravel aggregate (left, C100/115), high strength concrete with crushed aggregate (centre, C100/115) and schema of the fracture mechanism (right).

show that the ratio A representing uniaxial tensile strength over splitting tensile strength lies between approx. 1.1 and 1.3 for normal strength concrete. In contrast to this, for high strength concrete a ratio A from approx. 0.8 to 1.1 was determined (see Fig. 4). According to the data of CEB-FIP Model Code 90 (1993) the ratio A is about 0.9 assuming that the quotient of uniaxial tensile strength and splitting tensile strength does not depend on the concrete strength. Investigations of Remmel (1994) resulted in a quotient of A = 0.95, whereas the Norwegian standard recommends a factor of A = 0.667 (NS 3473 1989). The widespread spectrum of the suggested A-values, which were determined by means of experimental data (e.g. Bonzel 1964, Rocco et al. 2001), as well as the present experimental results allow the assumption, that the ratio of uniaxial tensile strength to splitting tensile strength depends not only on concrete strength, but also significantly on the geometry of the specimens and the aggregate used.

The obtained results indicate that concrete with crushed aggregate and similar matrix composition achieves a splitting tensile strength up to 15% higher than gravel concrete.

The fracture images of the splitting tension test specimens with variable compressive strengths point to differing fracture mechanisms. While normal strength concretes failed by a vertical crack in the centre line of the cross-section in conjunction with a wedge rupture below the load bearing strips (see Fig. 5), high strength concretes (see Fig. 6)

showed an increased crack formation in the areas of compressive stresses.

3 NUMERICAL INVESTIGATIONS

3.1 *Simulations*

The numerical simulations were carried out using the finite element code ATENA which contains a realistic approach for concrete failure at biaxial stress conditions. The essential relations were implemented according to Kupfer (ATENA 2000).

To ensure a realistic simulation of crack initiation and propagation, the cohesive crack model was employed. From all available cohesive crack models, the "Crack Band Model" developed by Bažant and Oh was selected and combined with the so-called "Fixed Crack Concept" to consider the direction of cracking (ATENA 2000). According to this concept, the direction of an initiated crack within an

Table 1. Overview of material parameter combinations for the numerical simulations.

Material parameter combination	A	B	C	D
$f_{c,cube}$ [MPa]	30	50	90	110
$f_{c,cyl}$ [MPa]	27	46	85	103
f_{ct} [MPa]	2.5	3.6	4.9	5.6
E_c [MPa]	28,000	32,000	40,000	45,000
G_F [N/m]	95	130	150	170
Poisson´s number [-]	0.2	0.2	0.2	0.2

Table 2. Overview of parameter combinations for the simulation of the splitting tension tests.

Parameter	Value/combination
D/H [mm/mm]	150/300, 75/150
Load bearing strip width b [mm]	5, 10, 20
ratio b/D	0.03, 0.07, 0.13
Material combination	A, B, C, D

element remains fixed during the entire crack expansion. This concept has the advantage that inactive cracks, which opened in an earlier "load step" and closed again afterwards, can be reactivated.

The employed material parameters for the FE computation (see Table 1) were determined according to the wide spectrum of the experimental investigations.

Parameter combinations for the splitting tension test simulations resulted from the three different load bearing strip widths b = 5, 10 and 20 mm, the four concrete material parameter combinations A, B, C and D (see Table 2) and the two different sized cylinders with D/H = 150/300 mm/mm and D/H = 75/150 mm/mm (see Fig. 7). For both cylinder geometries, the proportion of grid refinement and sample dimensions was held constant. In the area of load introduction and in the centre of the specimen, a finer grid discrimination was chosen. Thus the triangular finite element lengths were selected to be between 4 and 20 mm for the cylinders with D/H = 150/300 mm/mm and between 2 and 5 mm for the cylinders with D/H = 75/150 mm/mm.
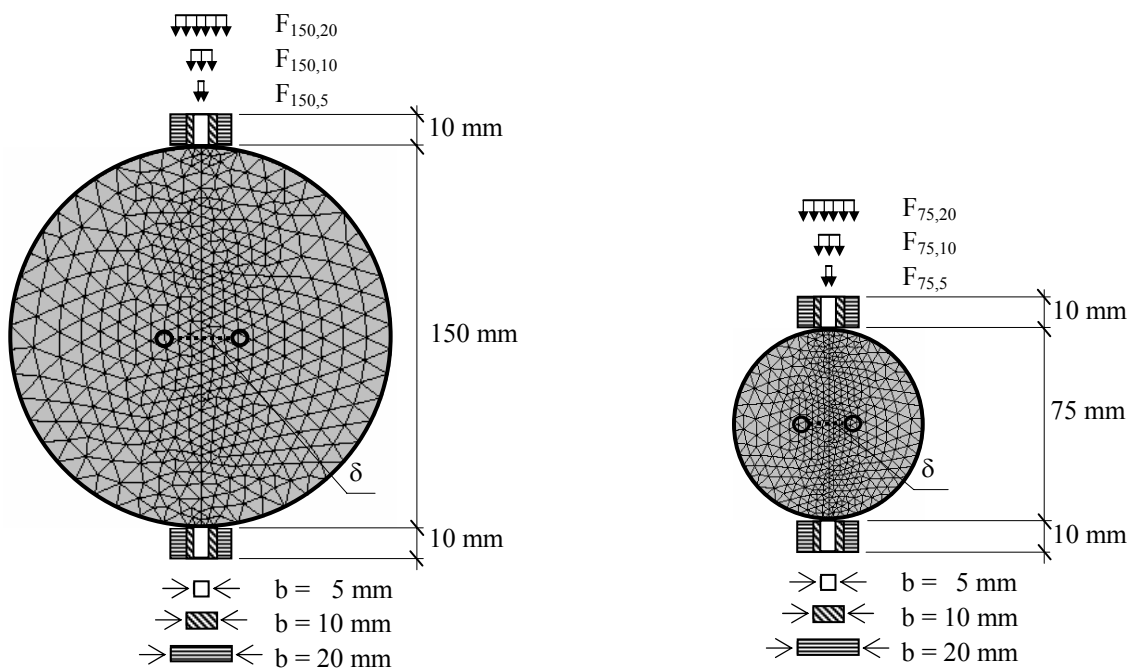
For the simulation of the uniaxial tension tests

Figure 7. FE-models for the simulation of the splitting tension tests: D/H = 150/300 mm/mm (left), D/H = 75/150 mm/mm (right).
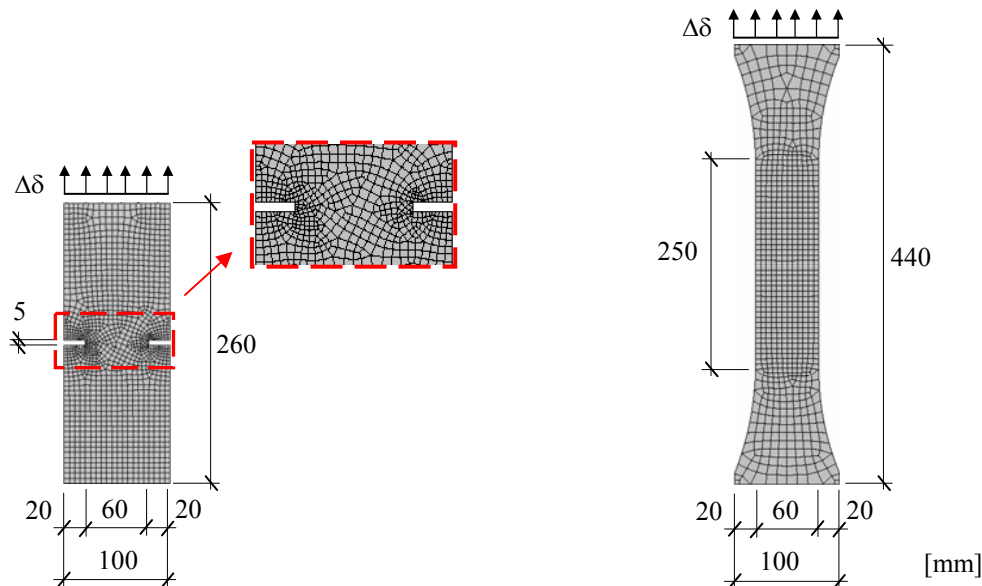

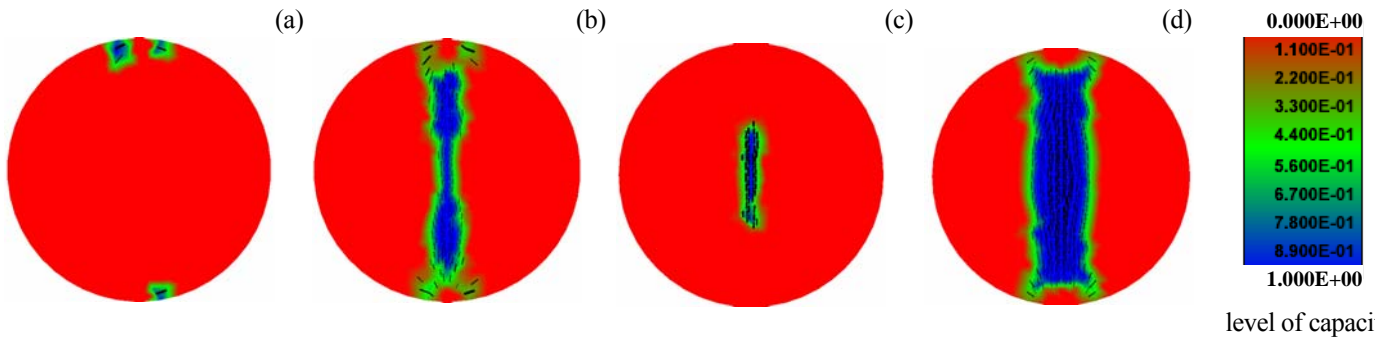Figure 8. FE-models for the simulation of the uniaxial tension tests.

Figure 9. Level of capacity (colours) and crack expansion (lines) for material combination A with b/D = 0.03 (a, b) and b/D = 0.13 (c, d).

both notched and dog-bone shaped prism meshes were generated (see Fig. 8).

Similar to the numerical splitting tension test, a finer FE grid was discretised in the expected zones of a possible crack process. In the case of the notched prisms, the length of the square finite elements was in between 4 to 10 mm.

For the simulation of the splitting tension tests as well as the uniaxial tension tests the FE grids were optimised regarding type and size of the finite elements and were chosen to meet the convergence criteria over a long simulated time span in order to record the softening curve of the stress-deformation behaviour.

3.2 *Results of the numerical simulations*

The numerical splitting tension tests revealed, that with decreasing concrete strength, the compressive stresses in the vicinity of the induced load, approach the compressive strength for b/D = 0.03 - 0.07. In the case of normal strength concrete those stresses even reach the compressive strength. As a consequence, the crack initiation in normal strength concrete is located in the area where high compressive stresses prevail (area of load introduction), instead of in the central areas of the specimen, where tensile stresses occur (see Fig. 9). Figures 9a, b show crack initiation and extension in a normal strength concrete with b/D = 0.03. Crack initiation starts in the area of compressive stress directly beneath the load bearing strips. The cracks then coalesce and propagate towards the centre of the specimen. Figures 9c, d show the simulation of crack formation for b/D = 0.13. Here, the crack initiation originates in the centre of the specimen where tensile stresses dominate.

Moreover, the numerical results show a strong size-effect. With increasing sample dimensions, the calculated values of splitting tensile strength decrease. This tendency could be noticed even for the same ratio of load bearing strip width to cylinder diameter (b/D = 0.07 and 0.13) (see Fig. 10).

The results of the numerical tension tests were in good agreement with the experiments.

4 COMPARISON OF EXPERIMENTAL AND NUMERICAL RESULTS

Figure 11 illustrates the relation between the concrete compressive strength f_c and the ratio A of uni-

D/H = 150/300 mm/mm,
b = 10 mm, b/D = 0.07
● —— $f_{ct,sp} = 2.30 \cdot \ln(f_c) - 5.50$
b = 20 mm, b/D = 0.13
▲ – – $f_{ct,sp} = 2.32 \cdot \ln(f_c) - 4.90$

D/H = 75/150 mm/mm,
b = 5 mm, b/D = 0.07
◆ – · – $f_{ct,sp} = 2.89 \cdot \ln(f_c) - 7.60$
b = 10 mm, b/D = 0,13
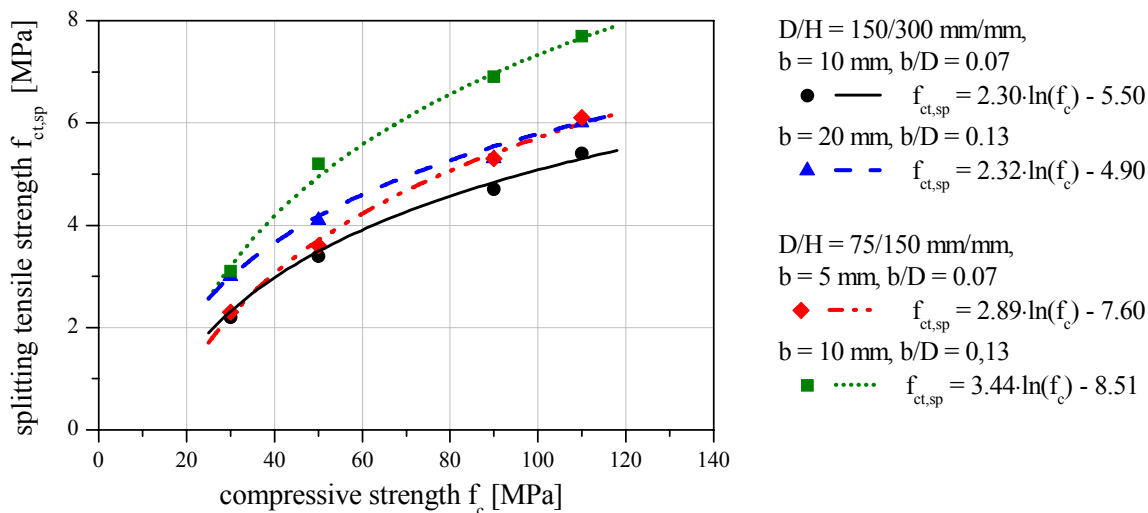■ ······ $f_{ct,sp} = 3.44 \cdot \ln(f_c) - 8.51$

Figure 10. Influence of specimen dimension and load bearing strip width on the numerically calculated splitting tensile strength (symbols); the curves show the corresponding fits.
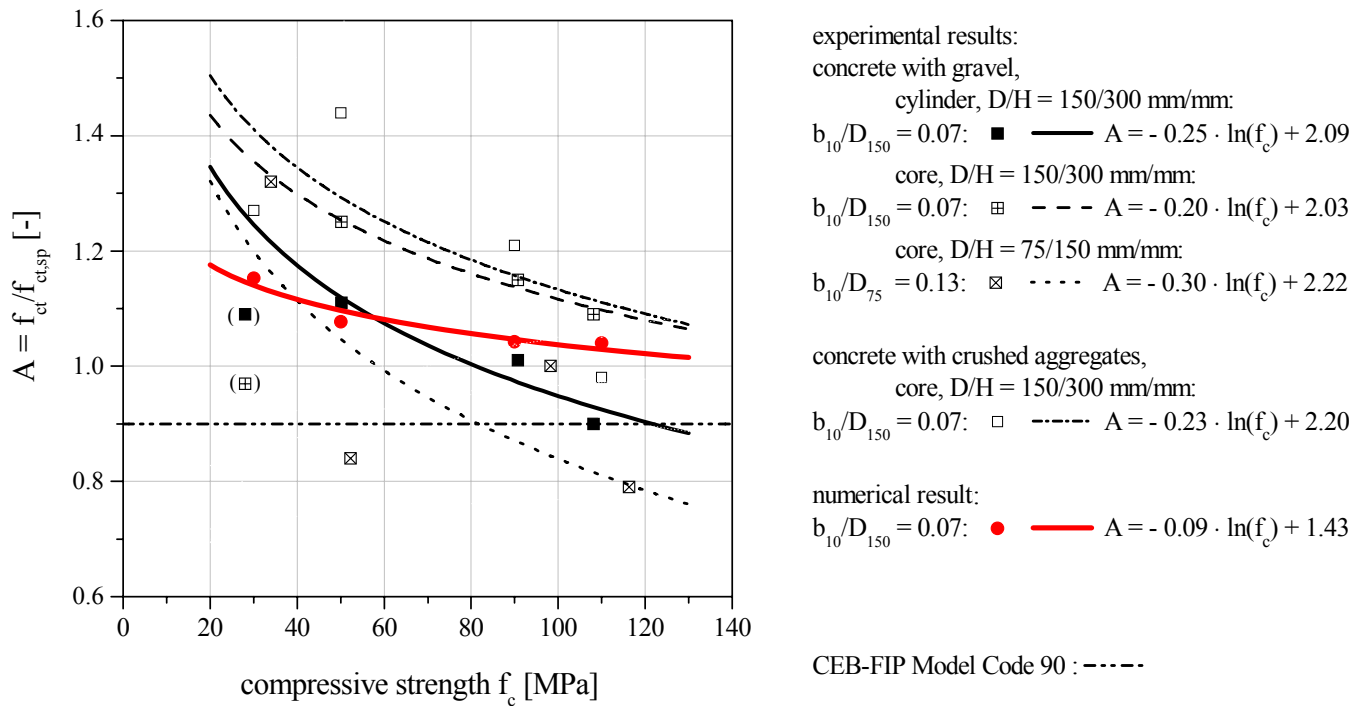
Figure 11. Comparison of numerically and experimentally determined relation of uniaxial tensile strength f_{ct} and splitting tensile strength $f_{ct,sp}$ in dependence of cylinder compressive strength f_c.

axial tensile strength f_{ct} to splitting tensile strength $f_{ct,sp}$. The wide spectrum of the experimentally obtained results could be confirmed by the numerical investigations.

For the following exemplary validation of the numerical model, the experimental results of the splitting tension tests on cylinders with b/D = 0.07 and 0.13 are selected.

The ratio A of the cylindrical test specimens consisting of gravel concrete with b/D = 0.07, differs to some extend from the numerically obtained relation (models with the same b/D ratio of 0.07), however, the tendencies are in accordance. The numerical results underestimate the A-value for normal strength concretes and overestimate it for high strength concretes. It is obvious, that for none of the concrete types used in this study a constant conversion factor like the one proposed in CEB-FIP Model Code 90 (1993) is valid. The above mentioned cases rather show an asymptotic behaviour towards this constant with rising compressive strength.

The determined splitting tensile strength values $f_{ct,sp}$ according to DIN EN 12390-6 (2001) (see Eq. 1) can be converted with good agreement into uniaxial tensile strength f_{ct} using logarithmic equations (see Fig. 11). However, these equations strongly depend on the sample dimensions, the ratio b/D as well as the used aggregates. Regarding specimens with gravel aggregate cast in cylindrical moulds with D/H = 150/300 mm/mm and b/D = 0.07, the experimentally obtained conversion formula in Equation 2 is in a reasonable agreement with the numerically derived correlation, in particu-

lar for usual structural concretes (f_c = 30 … 80 MPa).

$$f_{ct,sp} = \frac{2 \cdot F_u}{\pi \cdot D \cdot l} \qquad (1)$$

where $f_{ct,sp}$ = splitting tensile strength [MPa], F_u = measured peak load [N], D = diameter of specimen [mm] and l = length of specimen [mm].

$$A = \frac{f_{ct}}{f_{ct,sp}} = -0.25 \cdot \ln(f_c) + 2.09 \qquad (2)$$

where f_{ct} = uniaxial tensile strength [MPa] and $f_{ct,sp}$ = splitting tensile strength [MPa].

5 CONCLUSION AND OUTLOOK

The experimental investigations revealed, that with increasing compressive strength f_c the ratio of uniaxial tensile strength f_{ct} to splitting tensile strength $f_{ct,sp}$ decreases.

Both experimental and numerical test results show, that the uniaxial tensile strength f_{ct} cannot be computed from the splitting tensile strength $f_{ct,sp}$ on the basis of a single constant conversion factor. Furthermore, a single conversion formula that is independent of material properties, is unlikely to be found. Possible explanations are manifold. One main reason lies in the failure mechanism of the splitting tension test. It is affected by the concrete strength, sample dimensions and the ratio of load bearing strip width to cylinder diameter. Not only these individual effects but rather their combination

plays a substantial role and affects the material behaviour during the splitting tension test. A detailed description of the related processes including methods of fracture mechanics is the target of a current research project at the Institute of Concrete Structures and Building Materials of the University of Karlsruhe.

ACKNOWLEDGEMENT

REFERENCES

Arbeitsausschuss DIN 1048. 1991. *Prüfung von Beton – Empfehlungen und Hinweise als Ergänzung zu DIN 1048*. Schriftenreihe des DAfStb: 26. Berlin: Beuth.

Arıoğlu, N., Girgin, Z.C. & Arıoğlu, E. 2006. Evaluation of ratio between splitting tensile strength and compressive strength for concretes up to 120 MPa and its application in strength criterion. *ACI Materials Journal*, Vol. 103, No. 1: 18-24.

ATENA. 2000. *PROGRAM DOCUMENTATION*. Part 1, Theory. Prague.

Bonzel, J. 1964. Über die Spaltzugfestigkeit des Betons. *Beton*, Heft 4: 108-114.

CEB-FIP MC 90. 1993. COMITÉ EURO-INTERNATIONAL DU BÉTON: *CEB-FIP Model Code 1990*, Bulletin D'Information, No. 213/214. Lausanne: Thomas Telford Services Ltd.

DIN EN 12390. 2001. *Prüfung von Festbeton*. Berlin: Beuth.

DIN 1045-1:2001-07. 2001. *Tragwerke aus Beton, Stahlbeton und Spannbeton*. Teil 1: Bemessung und Konstruktion. Berlin: Beuth.

NS 3473. 1989. *Concrete Structures*, Design Rules. Oslo.

Remmel, G. 1994. *Zum Zug- und Schubtragverhalten von Bauteilen aus hochfestem Beton*. Schriftenreihe des Deutschen Ausschusses für Stahlbeton, Heft 444. Berlin: Beuth.

RILEM CPC 7. 1975. *Direct Tension*. Final Recommendation. E&FN Spon.

Rocco, C., Guinea, G.V., Planas, J. & Elices, M. 1999a. Size effect and boundary conditions in the Brazilian test: Experimental verification. *Materials and Structures*, Vol. 32: 210-217.

Rocco, C., Guinea, G.V., Planas, J. & Elices, M. 1999b. Size effect and boundary conditions in the Brazilian test: Theoretical analysis. *Materials and Structures*, Vol. 32: 437-444.

Rocco, C., Guinea, G.V., Planas, J. & Elices, M. 2001. Review of the splitting-test standards from a fracture mechanics point of view. *Cement and Concrete Research* 31: 73-82.

Zegler, C. 1956. Ein neues Verfahren zur Bestimmung der Betonzugfestigkeit. *Beton- und Stahlbetonbau*, Band 51, Heft 6: 139-140.